Separation Science and Technology
Publication details, including instructions for authors and subscription information:
http://www.informaworld.com/smpp/title~content=t713708471

Influence of the Si/Al Framework Ratio on the Microporosity of Dealuminated Mordenite as Determined from N_2 Adsorption

M. A. Hernández[a]; V. Petranovskii[b]; M. Avalos[b]; R. Portillo[c]; F. Rojas[d]; V. H. Lara[d]
[a] Departamento de Investigación en Zeolitas y Posgrado de Ciencias Ambientales del Instituto de Ciencias de la Universidad Autónoma de Puebla, México, Complejo de Ciencias, Ciudad Universitaria, Puebla, México [b] Centro de Ciencias de la Materia Condensada, UNAM, Ensenada, B.C. Mexico [c] Facultad de Ciencias Químicas, Universidad Autónoma de Puebla, Puebla, Mexico [d] Departamento de Química, Universidad Autónoma Metropolitana-Iztapalapa, México D.F.

To cite this Article Hernández, M. A. , Petranovskii, V. , Avalos, M. , Portillo, R. , Rojas, F. and Lara, V. H.(2006) 'Influence of the Si/Al Framework Ratio on the Microporosity of Dealuminated Mordenite as Determined from N_2 Adsorption', Separation Science and Technology, 41: 9, 1907 — 1925
To link to this Article: DOI: 10.1080/01496390600674901
URL: http://dx.doi.org/10.1080/01496390600674901

Separation Science and Technology, 41: 1907–1925, 2006

ISSN 0149-6395 print/1520-5754 online
DOI: 10.1080/01496390600674901

Influence of the Si/Al Framework Ratio on the Microporosity of Dealuminated Mordenite as Determined from N_2 Adsorption

M. A. Hernández
Departamento de Investigación en Zeolitas y Posgrado de Ciencias Ambientales del Instituto de Ciencias de la Universidad Autónoma de Puebla, México, Complejo de Ciencias, Ciudad Universitaria, Puebla, México

V. Petranovskii and M. Avalos
Centro de Ciencias de la Materia Condensada, UNAM, Ensenada, B.C. Mexico

R. Portillo
Facultad de Ciencias Químicas, Universidad Autónoma de Puebla, Puebla, Mexico

F. Rojas and V. H. Lara
Departamento de Química, Universidad Autónoma Metropolitana-Iztapalapa, México D.F.

Abstract: Dealuminated mordenites depicting SiO_2/Al_2O_3 molar ratios in the range 10-206 were analyzed through adsorption methods. The Type I-IV hybrid shape of the N_2 adsorption isotherms at 76 K on dealuminated mordenites indicated rather high micropore contents, though some amount of mesopores of slit-like geometry was also present. Micropore volumes and sizes were measured through α_S, t, and DA-plots, as well as by the NLDFT approach. Results indicated that mordenite

Received 6 October 2005, Accepted 26 February 2006
Address correspondence to M. A. Hernández, Departamento de Investigación en Zeolitas y Posgrado de Ciencias Ambientales del Instituto de Ciencias de la Universidad Autónoma de Puebla, Edificio 76, Complejo de Ciencias, Ciudad Universitaria, CP Puebla, 72570, Puebla, México. E-mail: mighern@siu.buap.mx

dealumination caused micropore opening and widening as well as the emergence of further slit-like mesopores; even though a slight structural collapse toward creation of mesopore zones occurred at high dealumination extents.

Keywords: Dealuminated mordenite, high-resolution α_s plots, supermicropores, ultramicropores, Dubinin-Astakhov

INTRODUCTION

The adsorption extent of volatile molecules on the surface of porous materials depend both on the characteristics of these molecules as well as on the chemical nature and geometrical properties of the adsorbent network such as pore shape, pore size, and number of interconnection paths between voids. In the case of adsorption taking place inside micropores smaller than twice the diameter of the adsorbate molecule, the enhancement of the adsorption energy is due to the overlapping between the potential fields emanating from both sides of the pore walls. Under this circumstance, a mechanism labeled as micropore volume filling takes place (1). Due to this enhanced adsorption attribute in comparison to mesoporous adsorbents, many solids with pores of molecular dimensions (micropores) are often used as selective adsorbents in industrial applications. Among microporous adsorbents activated carbon fibers, microporous silica, and zeolites are particularly relevant (2). Synthetic zeolites of the types LTA, Y, MOR and ZSM-5 are outstanding adsorbents by reason of their exceptional textural characteristics.

The structure of mordenite (MOR framework type) is characterized by an orthorhombic unit cell. Parameters of the simple mordenite cell correspond to $a = 1.8052–1.8168\,\text{nm}$, $b = 2.0527\,\text{nm}$, $c = 0.7501–0.7537\,\text{nm}$, $\alpha = \beta = \gamma = 90^\circ$. The Si/Al molar ratio is found between 4.5 and 5.5. Mordenite depicts two types of hollow channels: the first one (channel A) consisting of 12-membered rings each of which having 12 oxygen molecules and running parallel to the [001] plane or c axis and possessing a free access of $0.65 \times 0.7\,\text{nm}$, and the second one (channel B) being a distorted 8-membered ring channel running along the same [001] plane with a window aperture of $0.26 \times 0.57\,\text{nm}$ (Fig. 1) (3). Channels A and B are interconnected via perpendicular 8-membered channel B tubes, in the form of small side pockets along the [010] axis. Thus the mordenite channel system is essentially a 2-dimensional network with elliptical 12-ring apertures and a *limiting diffusion* in the [010] or b direction. The mordenite channel structure can be visualized in Fig. 1. Cation sites reside in the centers of the 8-membered rings that are parallel either to c or b, these sites are regularly occupied thus leading to pore blocking and leaving the 12-membered channels as the only ones for molecular diffusion. It has been observed that mordenite allows the passage of molecules not greater than 0.42 nm.

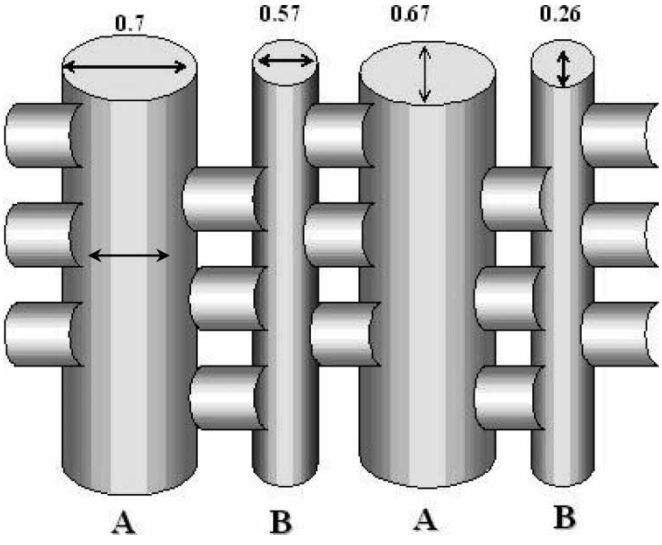

Figure 1. Schematic representation of the pore channels in the mordenite structure. The dimensions of pore channels are in nm.

Adsorption isotherm analysis has provided supporting evidence for the incidence of two stages of micropore filling (4):

a. A *primary* process involving enhanced adsorbent-adsorbate interactions in pores of molecular dimensions (i.e., *ultramicropores*: voids smaller than 0.7 nm); and
b. A cooperative (*secondary*) process taking place in wider micropores (i.e. *supermicropores*: voids between 0.7 and 2 nm) by means of the cohesion forces that are developed between the adsorbed molecules.

The limiting width for primary micropore filling seems to be little more than two molecular diameters of the adsorptive molecule. Thus, the upper pore size limit for primary micropore filling by nitrogen is $\sim$0.7–0.8 nm (i.e., ultramicropores). The upper limit for secondary micropore filling depends on the adsorbate-adsorbate interactions and is probably in the region of five molecular diameters ($\sim$2 nm for nitrogen). Having these limits in mind; N_2 primary micropore filling usually finishes at relative pressures (p/p^0, where p^0 is the saturation vapor pressure of the adsorptive) well before 0.01, at which point supermicropore filling is already taking place.

In a zeolitic framework, neighboring tetrahedral Al^{3+} and Si^{4+} species share the oxygen atoms that surround them and therefore these ions are not directly exposed to the sorbate molecules. Consequently, the main interactions of the adsorbate molecules with a zeolite structure occur through lattice oxygen

atoms and extra framework cations. Partially dealuminated zeolites have special properties such as enhanced hydrothermal stability, and excellent catalytic activity for cracking, hydrocarbon synthesis, and isomerization. For these reasons, over many years zeolites have attracted the interest of numerous researchers. A dealumination process of zeolitic substrates, by either hydrothermal treatment or acid leaching, modifies their innermost structure sometimes more than direct chemical exchanges with, for instance, $SiCl_4$ or $(NH_4)_2SiF_6$. It is generally accepted that steaming induces the removal of Al atoms from the zeolitic framework and gives rise to extra-framework Al^{3+} species, which are more or less bounded to oxygen atoms and/or hydroxyl groups. The vacancies created by the removal of tetra-coordinated Al atoms are filled by Si atoms coming from other parts of the zeolite. When a large number of Si atoms have left a given area of the zeolite, the structure can suffer cracks or even collapse. This leads to the formation of an important secondary porosity (i.e., mesopores are created) with a wide distribution of sizes (5). It is therefore necessary to employ characterization techniques such as N_2 adsorption-desorption, Hg porosimetry, and electron microscopy in order to detect these emergent mesopore sizes. Other analysis techniques have also been used for characterizing dealuminated zeolites, *e.g.* IR spectroscopy and X-ray diffraction, as well as solid-state NMR by observation of ^{29}Si, ^{27}Al, ^{1}H, and adsorbed ^{129}Xe nuclei (6). Springuel et al. (7) have performed useful studies on the properties of dealuminated zeolites. The adsorption capacity of a zeolite has been found to be a function of the Si/Al ratio (8). Zeolites enriched in Al are hydrophilic and show little selectivity toward organic molecules, whilst high-silica zeolites are hydrophobic and tend to attract more strongly the organic compounds (9).

In this work, it will be shown that a partial destruction of the zeolitic microstructure by a dealumination process can alter the sorption characteristics of the pore network by:

1. Expanding the micropore volume accessible to the adsorptive molecules;
2. Widening the micropore sizes; and
3. Creating larger voids (mesopores).

Therefore, it should be of great scientific and practical interest to explore the adsorption properties of dealuminated mordenites through different adsorption methods of analysis.

In this paper, we report the results of a detailed experimental study of N_2 adsorption equilibrium on dealuminated mordenites. The structural parameters of these porous substrates such as surface area, micropore volume, and (when possible) micropore size are calculated through different methods. With these objectives in mind, N_2 adsorption isotherms at 76 K on dealuminated mordenites have been carefully measured by means of a volumetric static technique.

The manuscript is organized as follows. The experimental details are given immediately below. These include materials, description of characterization techniques, and measurement of N_2 adsorption isotherms by a volumetric instrument. Next, several methods of analysis of pore structural parameters are succinctly described in order to calculate important structural parameters, followed by a discussion of the characterization results, and finally relevant conclusions are delivered.

EXPERIMENTAL SECTION

Materials

A set of dealuminated mordenites (MOR) with SiO_2/Al_2O_3 molar ratios (MR) varying from 10 to 206 were supplied by TOSOH Corp., Japan, in a protonated (H^+-MOR) form. These products were used as received and were not subjected to further chemical processes. Through the text and figures, mordenite samples are labeled as HM followed by the appropriate MR value, e.g. HM (10, 15, 20, 30, 72, 110, 128, and 206). Ultrahigh purity gases N_2 and He (>99.999%, INFRA Corp.) were employed for the textural sorption studies of dealuminated mordenites.

XRD Measurements

X-ray diffraction patterns were determined by means of a Siemens D-500 diffractometer that employs a nickel-filtered Cu-Kα radiation.

N_2 Sorption

N_2 adsorption measurements were performed at the boiling point of liquid nitrogen (76 K at the 2250 m altitude of Puebla, México) in an automatic volumetric adsorption instrument (Autosorb-1, Quantachrome Instruments). N_2 adsorption isotherms were determined in the p/p^0 interval extending from 0.02 to 0.995; in turn, high resolution N_2 isotherms were measured for some selected samples in the $10^{-5} - 0.995$ p/p^0 range. The adsorptive (N_2) saturation pressure, p^0, was continuously registered during the course of the adsorption-desorption measurements. Prior to the sorption experiments, samples were outgassed at 623 K during 20 hours under turbomolecular pump vacuum at a pressure lesser than 10^{-6} Torr.

Calculation Methods

The BET (10), Langmuir (11), and *t*-plot (external) surface areas (12) of the series of mordenites under study were evaluated from N_2 adsorption data in the p/p^0

range extending from 0.04 to 0.2. The total pore volume, V_{Σ}, was estimated through the Gurvitsch Rule (13) on the basis of the volume adsorbed at a relative pressure $p/p^0 \approx 0.95$ and calculated as volume of liquid. The microporous volume inherent to our mordenites was determined by:

a. Sing α_s-plots (14);
b. *t*-plots (15);
c. The classical Dubinin-Astakhov (DA) procedure (16); while
d. Supermicropore sizes were determined for selected samples through the Non-Local Density Functional Theory (NLDFT) approach (17).

For calculating micropore volumes from the α_S -plot method, a typical α_S range corresponding to p/p^0 values between 0.04 and 0.7 was considered. In turn, for the high- resolution α_s-plots, a p/p^0 range of 10^{-5}–10^0 was utilized. For setting up these typical and high-resolution α_S plots, a N_2 isotherm on a non-porous silica sample (13) was chosen as reference.

In order to construct the *t*-plots, it was necessary to calculate the thickness, *t* (nm), of the adsorbed layer of N_2 as function of p/p^0, here this was performed by means of the Frenkel-Halsey-Hill (FHH) (13) equation:

$$t\ (\mathrm{A}) = 3.54\left[\frac{5}{\ln(p^0/p)}\right]^{1/3} \tag{1}$$

The Dubinin-Astakhov (DA) treatment that was employed for calculating mordenite microporous volumes is based on the following equation:

$$W = W_0 \exp\left[-\left(\frac{A}{\beta E_0}\right)^n\right] \tag{2}$$

where *W* is the microporous volume that have been filled at a given p/p^0 and W_0 is the total volume of the microporous space; in turn $-A = RT \ln (p^0/p)$ is the negative of the isothermal molar Gibbs free energy of transfer from the liquid, at temperature *T* and saturation pressure p^0, to the adsorbate phase at equilibrium pressure $p\beta$ is called a scaling factor and E_0 is the characteristic energy of the adsorption system and reflects the influence of the nature of the substrate on the adsorbed amount.

It should be mentioned that the DA equation is applicable for describing the adsorption of gases and vapors on energetically uniform micropores. Since the dealuminated mordenites studied in these work possess relatively minute structural heterogeneities (according to the X-ray diffraction patterns), equation (2) is expected to render a good estimation of the total micropore volume. A DA plot can be constructed by plotting ln *W* vs. $\ln^n(p^0/p)$. In the case of truly microporous materials, a DA plot often exhibits a linear region extending over a wide range of relative pressures (e.g. $10^{-5} - 0.2$) and W_0 can be calculated from the intercept. A DA plot requires adsorption data to be corrected for meso and macropore adsorption, which would have

contributed to the uptake at lower relative pressures. This correction could be made if the external surface area, A_{St}, as well as the thickness of the adsorbed layer (as function of p/p^0) are known.

The Non-Local Density Functional Theory (NLDFT) (17) has been designed to account for the pore sizes in voids of well–defined geometry. In this approach the molecules adsorbed in the pores tend to pack according to adhesion forces established with the substrate (i.e. attractive forces between adsorptive and adsorbent molecules) and interactions with the remaining fluid molecules. The molar density of the adsorbed phase varies as a function of pore size. An adsorption isotherm is calculated on a given pore shape (spherical, cylindrical, slit-like, etc.) and the experimental isotherm is given as the sum of a number of individual single-pore isotherms multiplied by their relative abundance over a range of pore sizes. In the present case, the microporous structure of mordenite can be approximated as a bundle of parallel cylindrical pores and the nature of the adsorbent can be assumed as that of silica. In this way, a supermicropore size distribution of the mordenitic adsorbents can be calculated from high-resolution adsorption isotherms.

RESULTS AND DISCUSSION

X-ray Analysis

The XRD patterns of all samples (Fig. 2) are typical of mordenite zeolites as described by Treacy et al. (18). In general, all mordenite zeolites exhibited reasonable sharp diffraction patterns and consequently good crystallinity. Nevertheless, the XRD patterns of samples HM128 and HM206 are affected to some extent and are not as sharp as those corresponding to the remaining mordenite specimens. Typical peaks of the mordenite crystalline structure appear at the following 2θ diffraction angle values: 6.5°, 8.7°, 9.8°, 13.5°, 15.3°, 19.8°, 22.5°, 25.8°, 26.5°, 27.7°, and 31.3°. A clear effect of the dealumination process can somewhat be visualized through the progressive diminution in intensity of the peak appearing at 6.5° in going from sample HM10 to HM128 (Fig. 2).

N_2 Adsorption

Nitrogen adsorption isotherms at 76 K on mordenites are shown in Fig. 3 (p/p^0 vs. adsorbed volume in cm^3 STP per gram of zeolite). The uptake capacity of dealuminated mordenites can be quantitatively inferred from this figure according to the value of the adsorbed volume at which the adsorption plateau is reached. Additionally, high-resolution N_2 adsorption isotherms on mordenites in a logarithmic p/p^0 scale in the range of p/p^0 between 10^{-5} and 10^0 are depicted in Fig. 4.

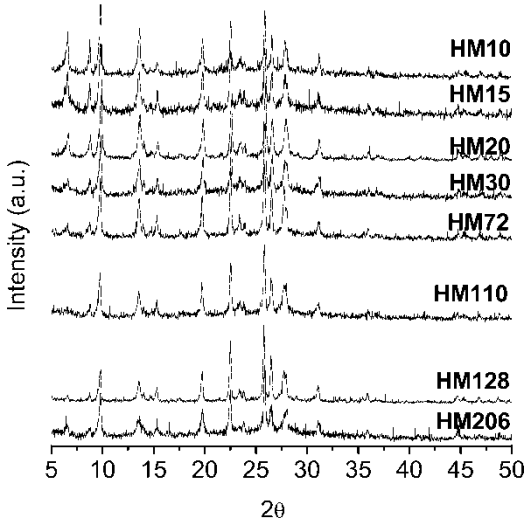

Figure 2. X-ray diffraction patterns of dealuminated mordenites.

The N_2 sorption isotherms of dealuminated mordenite (Fig. 3) are mostly Type I curves according to the IUPAC classification (20). Some of these isotherms (especially those that depict the higher dealumination extents) also include a non-negligible Type IV isotherm contribution. For all MOR samples, the C_B values proceeding from the BET equation are negative and this is a further indication of the microporous nature of the dealuminated mordenite substrates (12). It is also noteworthy to see that the plateau of each isotherm attains a characteristic height depending on the identity of the sample under analysis, although two things should be recognized (Table 1):

1. The total pore volumes (V_Σ) of all samples are not extremely different from each other (especially those of lowly dealuminated mordenites); and
2. The total pore volumes of highly dealuminated HM110 and HM128 samples are the bigger ones.

The primary (intense) process of ultramicropore filling in the mordenite samples is evident when observing the adsorbate uptake that occurs at low p/p^0 in the high-resolution N_2 isotherms shown in Fig. 4. It also manifests the existence of a secondary process of supermicropore filling due to the presence of a distinctive rounded knee in most of the N_2 isotherms. This knee can also indicate that some multilayer adsorption is taking place on mesopores, and on external surface of the samples (19). An additional

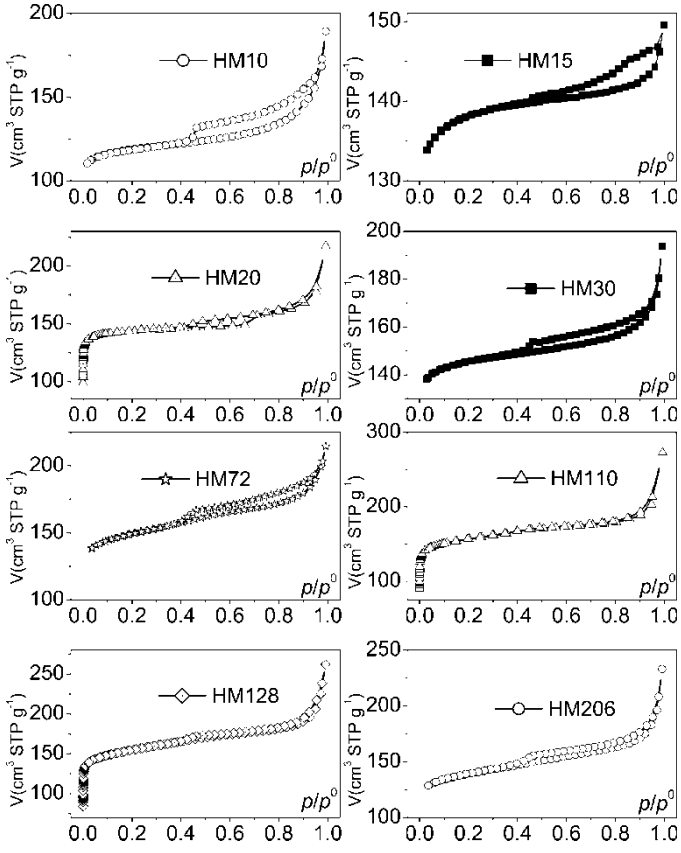

Figure 3. N_2 sorption isotherms at 76 K on dealuminated mordenites.

feature of dealuminated mordenite N_2 sorption isotherm shapes is the fact that, at intermediate and high p/p^0 values, the hysteresis loops become IUPAC Type H3 cycles, thus indicating the presence of slit-like pores (20) in the dealuminated zeolites.

Table 1 lists a series of values corresponding to some important pore structural parameters obtained from the analysis of the N_2 sorption isotherms, such as surface areas calculated from:

a. The BET model;
b. The Langmuir equation; and
c. α_S and *t*-plots. In the same table there appear other important parameters such as:
d. The C_B constant of the BET equation; and
e. The total pore volume, V_Σ, that was calculated according to the Gurvitsch rule (applied at $p/p^0 = 0.95$).

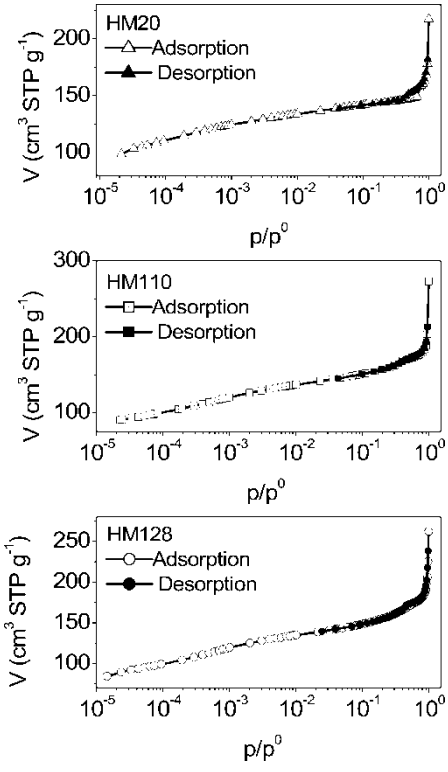

Figure 4. High-resolution N_2 sorption isotherms of selected dealuminated mordenite samples in a logarithmic p/p^0 scale.

The range of relative pressures that was chosen to calculate the BET parameters is also shown in Table 1. The total sorption capacities (i.e. V_Σ) of dealuminated mordenite substrata exhibit the following decreasing order: 110 > 128 > 72> 206 > 20 >30 >10> 15. The relatively smaller adsorption capacities of samples HM15 and HM10 can somehow be justified by the fact that these mordenites have been just subjected to a mild dealumination process and there exists a strong possibility that some bulky cations or impurities are blocking the entrance to the pore channels. In general, and since no general trend is followed within the above V_Σ sequence, it is evident that the adsorption capacity of our mordenite substrata has something to see with three concomitant processes: dealumination, micropore widening, and mesopore creation. While further evidence will be provided for these processes in the subsequent sections, it can still be advanced that the dealumination process can bring about the opening and widening of the existing supermicropores as well as the development of mesopore voids in the form of slit-like pores.

Table 1. Adsorption structural parameters of dealuminated mordenites

Mordenite zeolites	$A_{SB}\,m^2\,g^{-1}$	$A_{SL}\,m^2\,g^{-1}$	$A_{St}\,m^2\,g^{-1}$	$A_{\alpha S}\,m^2\,g^{-1}$	BET p/p^0 Range	C_B	$V_\Sigma\,cm^3\,g^{-1}$	W_0/V_Σ
HM10	397	534	49.5	53.5	0.085–0.18	−69.4	0.239	66.9
HM15	512	609	7.4	8.2	0.04–0.11	−224	0.222	94.6
HM20	553	634	24.0	26.9	0.02–0.09	−570	0.273	76.2
HM30	524	648	29.0	32.1	0.05–0.13	−164	0.259	82.2
HM72	526	686	38.7	42.6	0.05–0.16	−155	0.292	77.7
HM110	576	707	41.2	45.4	0.04–0.11	−382	0.328	70.4
HM128	558	683	46.4	52.5	0.05–0.13	−255	0.317	54.3
HM206	487	639	111	114	0.05–0.16	−147	0.281	58.7

As_B, is specific BET surface area; As_L is Langmuir specific surface area; As_t is external surface area calculated by the *t*-method; $A_{\alpha S}$ is surface area calculated by the αs-method; C_B is BET constant; p/p^0 is the relative pressure range used to construct the BET plots; V_Σ is the total pore volume determined close to saturation ($p/p^0 \sim 0.95$) and calculated as volume of liquid, W_0/V_Σ represents the degree of crystallinity of each sample.

Microporosity

Total micropore volumes (W_0, in $cm^3\,g^{-1}$) of dealuminated mordenites are listed in Table 2. These values have been calculated from:

1. α_s-plots;
2. *t*-plots; and
3. the D-A equation (in this last case by optimizing the values of the parameters *n* and E_0).

The ratio of the micropore-filling capacity to the total adsorption uptake $W_0/V\Sigma$, a parameter that somehow indicates the degree of crystallinity of the zeolite under analysis (21) is also included in Table 2. The micropore volumes reported in this work happen to be in good agreement with those reported for HY, HZSM5 and H-mordenite zeolites (22), and also with the results found for dealuminated offretites (23).

For constructing the α_S plots, a standard N_2 adsorption isotherm on non-porous silica (13, 24) needs to be employed as the reference material. Selection of this non-porous sample (13) was based on the fact that adsorption on this substrate occurs as on a flat surface. As seen in Table 2, *t*-plots provided slightly different total micropore volumes if compared to those proceeding from α_S-plots since, in the former case, the thickness of the adsorbed layer was calculated through an FHH isotherm equation instead of the employment of a non-porous silica standard.

A high-resolution α_s-plot for the HM110 dealuminated mordenite is shown in Figs. 5a–5b. Note that in this plot there exist two linear regions:

1. One occurs at low p/p^0 (α_s) values; and
2. Another one appears at high p/p^0 values.

Table 2. Total micropore and mesopore volumes of dealuminated mordenites calculated through different methods of analysis

Mordenite	α_s	*t*	DA	*n*	E_0 kJ/mol	V_{meso}
10	0.160	0.157	0.190	1.0	21.0	0.079
15	0.210	0.210	0.220	1.4	19.2	0.012
20	0.208	0.206	0.220	2.3	11.1	0.065
30	0.213	0.212	0.230	1.0	24.4	0.046
72	0.227	0.226	0.250	1.0	15.1	0.065
110	0.231	0.163	0.240	1.8	9.5	0.097
128	0.172	0.171	0.230	2.1	9.3	0.145
206	0.165	0.157	0.230	1.0	15.2	0.116

α_s is Sing's α_s method, *t* is the *t*-plot employing the FHH adsorption equation, DA represents the Dubinin-Astakhov equation, E_0 is characteristic energy of adsorption, V_{meso} is calculated by subtraction of $W_{0\alpha\ S}$ from V_Σ (Table 1).

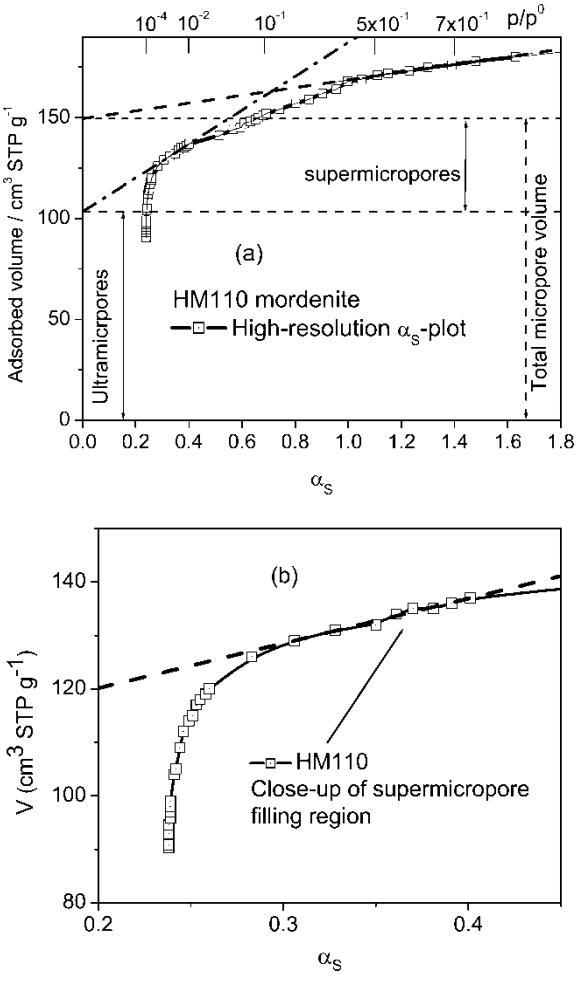

Figure 5. (a)High-resolution α_s-plot for N_2 adsorption on dealuminated HM110 mordenite, showing the ultramicropore and supermicropore volume regions; (b) close-up of the supermicropore linear region High-resolution α_s-plot for N_2 adsorption on dealuminated HM110 mordenite.

The first of these linear regions (Fig. 5b) can be identified with the supermicropore filling process (Fig. 5b), since ultramicropore (25) saturation has already been attained at these p/p^0 values; it is for this reason that the ultramicropore volume can be calculated from the intercept of the α_s-plot (see Fig. 5). The second region corresponds to the traditional calculation of total micropore volume, once that all micropores (ultramicropores + supermicropores) have been occupied with adsorbate. In Table 3, we have listed the α_s ultramicropore and supermicropore volumes corresponding to

Table 3. Ultramicropore (Um) and supermicropore (Sm) volumes of dealuminated mordenites calculated through the α_S (within the p/p^0 range shown in the square brackets) and the NLDFT methods of analysis

Mordenite	Sm-α_S	[p/p^0 range]	Sm-NLDFT	Um-α_S
HM20	0.033	[0.003,0.009]	0.023	0.175
HM110	0.071	[0.003,0.009]	0.054	0.160
HM128	0.011	[0.003,0.009]	0.049	0.161

samples for which high-resolution N_2 sorption isotherms were available. The extent of microporosity in dealuminated mordenites follows a very particular sequence (Table 2). First, the micropore volume starts increasing (from sample HM10 to sample HM15), afterward it remains almost constant, independently of the dealumination extent (samples HM15, HM20, HM72, and HM110), and to finally decrease when approaching the highest dealumination degrees (samples HM128, HM206).

An assessment about the extent of mesoporosity existing in dealuminated mordenites can be made by subtracting the micropore volume $W_{0\alpha S}$ from V_Σ (Table 2, V_{meso} column). From here it is possible to see that, in general, the mesopore volume increases with the degree of dealumination. The three samples that have suffered the highest dealumination extent (HM110, HM128, and HM206) show the highest mesopore volume thus indicating that, together with the H3 shape of the N_2 sorption hysteresis loops of these samples, that more and more cracks (i.e., pores between almost parallel walls) are being generated in the interior of the samples as the dealumination process is pursued.

Progressive dealumination has then rendered a special type of porous mordenites, in which micropores coexist altogether with mesopores. The cation channel blocking effects observed in these zeolites (e.g. HM10) are diminished through the dealumination treatment by lowering their cation-exchange capacity by leaching Al^{+3} from framework positions and introducing H^{+1} into the few remaining cation sites (26). Additionally, dealumination takes a role in the removal of amorphous glassy materials blocking the channels of the mordenite structure. In summary, dissolution of framework Al (which is a significant process) causes damages in the framework structure (i.e., gives rise to mesopores) concurrently with the micropore opening and lowering of the cation exchange capacity of the mordenite substrates.

NLDFT Pore Size Analysis

An approximate idea about what has happened with the sizes of the original mordenite elliptical openings (0.65×0.7 nm, A channels) could be

achieved through the NLDFT treatment (17) by assuming cylindrical channels. In contrast to A channels, the 0.26×0.57 nm (B channels) voids are expected to hinder the entrance of N_2 molecules. The secondary volume filling of mordenite A channels is equivalent to the accumulation of an adsorbed layer of between one and two molecular N_2 diameters. On the basis of the NLDFT approach, Table 3 and Figs. 6–8 provide a good idea about the actual width values and pore-size distributions of the supermicropore voids existing in the dealuminated mordenites for which high-resolution N_2 isotherms are available.

DA Plots

Table 2 lists the optimized W_0, n, and E_0 values of the DA equation related to N_2 adsorption on dealuminated mordenites. The DA results shown in Table 2 suggest that the chemical treatments applied to mordenitic zeolites favor the opening and widening of their micropores. Nevertheless, the microporous volumes calculated from the DA equation are somewhat different from the microporous volumes calculated by the t and α_S methods. The fact that these DA microporous volumes are always larger than the volumes calculated by the other methods suggests that the uptake at low relative pressures should be corrected for mesopore adsorption. This correction would result in a lower extrapolated value of the micropore volume from the DA equation, and a better agreement with the other (α_S and t) methods would be reached.

The DA pore volume size distribution, as compared with the results obtained from the NLDFT treatment with respect to sample HM110, can be seen in Fig. 8. There, it is possible to see that the DA treatment, although overestimating somehow the pore sizes, still provides an approximate estimation of micropore volumes and their corresponding pore sizes.

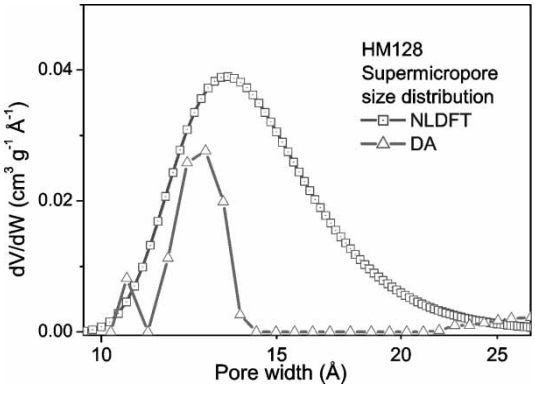

Figure 6. Supermicropore size distributions calculated from N_2 adsorption on the HM-128 dealuminated mordenite through the NLDFT and DA approaches.

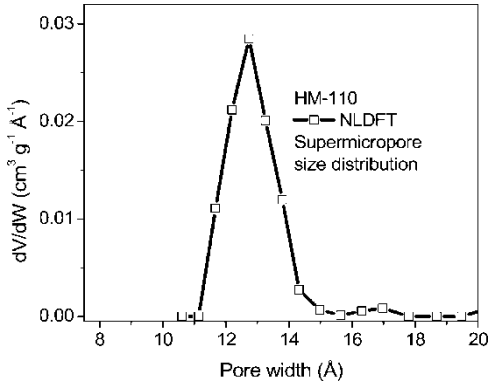

Figure 7. Supermicropore size distribution calculated from N_2 adsorption on the HM-110 dealuminated mordenite through the NLDFT approach. The NLDFT supermicropore volume of $0.054\,cm^3\,g^{-1}$ is not far from the corresponding value calculated through the α_S method ($0.071\,cm^3\,g^{-1}$).

A supplementary observation, concerning the DA characterization results, is that the larger E_0 values reported in Table 3 correspond to the HM10, HM15 and HM30 substrates. This effect on E_0 can be due to the greater energetic heterogeneity that is expected to exist in the lesser dealuminated samples. In general, the dealumination treatment diminishes the adsorption energy heterogeneity and this kind of approximate trend is observed in Table 2, with the possible exception of the HM20 and HM206 substrates.

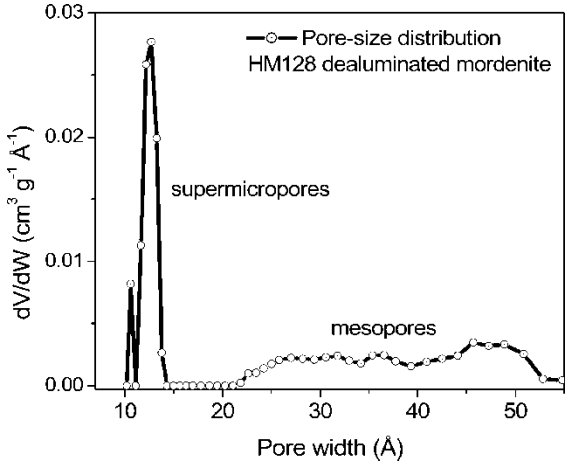

Figure 8. NLDFT Pore-size distribution of HM128 dealuminated mordenite showing supermicropore and mesopore regions.

Pore Structure Changes during Dealumination of Mordenite Samples

On the basis of the above characterization results, the following is a possible picture of what is happening with the pore structure of dealuminated mordenites:

- During the early stages of the dealumination process the pore volume is made accessible to the adsorptive molecules by the removal of some impurities or bulky ionic species that are blocking the micropore channel entrances. Table 2 shows the significant increase of micropore volume in going from sample HM10 to sample HM15.
- Mordenite A channels can accept the introduction of adsorbate molecules and seem to widen up as the dealumination procedure becomes more and more intense (see Figs. 7–8).
- Mesopores, in the form of slit-like pores (and likely promoted by the removal of matter through the dealumination process) develop steadily (see V_{meso} in Table 2) as the dealumination process is pursued. Fig. 8 shows the NLDFT supermicropore and mesopore sizes existing in HM128, where some of the micropore volume has disappeared in favor of a similar amount of mesoporous slit-like voids.

CONCLUSIONS

Synthetic mordenites depict a high crystallinity, which is somehow influenced by a dealumination treatment thus indicating the initial presence of a certain degree of contamination of the structure with amorphous glassy materials or clays. The presence of cations or mineral deposits blocking the pore channels of a mordenite, and the consequent perturbation of its crystalline structure, can reduce its sorption activity by making inaccessible the microporous volume to the adsorptive molecules. Dealumination of a high-silica mordenite can produce a more viable adsorbent. Ultramicropore and supermicropore contributions to the total micropore volume in a dealuminated mordenite can be evaluated through high-resolution α_s-plots. Slightly and highly dealuminated mordenites depict a hybrid Type I-Type IV isotherm quality; thus indicating the participation of both micropores (especially supermicropores) and slit-like mesopores in setting up the porous structure of dealuminated mordenites. Nevertheless, the partial damage (mesopores) that is produced in mordenites as consequence of the dealumination process is more intense in highly dealuminated substrates. The NLDFT approach renders reasonable pore sizes and pore volumes for dealuminated mordenites in some agreement with results proceeding from classical t, α_S, and DA methods.

ACKNOWLEDGEMENTS

Thanks are given to:

1. The Benemérita Universidad Autónoma de Puebla, México, (VIEP-BUAP) for financial support through grant II 118102; and
2. Consejo Nacional de Ciencia y Tecnología (CONACYT), Mexico through project 47631-F.

REFERENCES

1. Sing, K.S.W. (1995) In *Porosity in Carbons: Characterization and Applications*; Patrick, J.W. (ed.); Edward Arnold: London, U.K.
2. Matsumoto, A., Zhao, J., and Tsutsumi, K. (1997) Adsorption behavior of hydrocarbons on slit-shaped micropores. *Langmuir*, 13: 496.
3. Huddersman, and Klimczyk, M. (1996) Separation of hexane isomers on zeolites mordenite and beta. *J. Chem Soc. Faraday Trans.*, 92: 143.
4. Roberts, R.A., Sing, K.S.W., and Tripathi, V. (1987) Adsorption of nitrogen and neopentane vapor by microporous carbons. *Langmuir*, 3: 331.
5. Tsitsihvili, G.V., Andronikashvili, T.G., Kirov, G.N., and Filizova, L.D. (1992) *Natural Zeolites*; Ellis Horwood: Sussex, U.K.
6. Julbe, A.,De Menorval, L.C., Balzer, C., David, P., Palmeri, J., and Guizard, C. (1999) ^{129}Xe NMR investigations for the textural characterization of sol-gel derived amorphous microporous silica. *J. Porous Materials*, 6: 41.
7. Springuel, M.A. and Fraissard, J.P.A. (1992) ^{129}Xe NMR study of dealuminated mordenites. *Zeolites*, 12: 841.
8. Weber, G., and Simonot-Grange, M.H. (1994) Characterization of the dealumination effect into H faujasites by adsorption: Part 2. The hexane molecule as a pore volume probe. *Zeolites*, 14: 433.
9. Elaiopoulos, K. (2002 In *6th International Conference on the Occurrence, Properties and Utilization of Natural Zeolites*; Misaelides, P. (ed.); Thessaloniki: Greece.
10. Brunauer, S. (1945) *The Adsorption of Gases and Vapors*; Princeton University Press: Princeton, N. J.
11. Ruthven, D.M. and Kaul, B.K. (1993) Adsorption of aromatic hydrocarbons in NaX zeolite, 1. Equilibrium. *Ind. Eng. Chem. Res.*, 32: 2047.
12. Remy, M.J. and Poncelet, P.A. (1995) New approach to the determination of the external surface and micropore volume of zeolites from the nitrogen adsorption isotherm at 77 K. *J. Phys. Chem.*, 99: 773.
13. Gregg, S.J. and Sing, K.S.W. (1982) *Adsorption, Surface Area and Porosity*, 2nd ed.; Academic Press: London, U. K.
14. Sing, K.S.W. (1989) In *Third International Conference on Fundamentals of Adsorption*, Mersmann, A.B. and Scholl, S.E. (eds.); Engineering Foundation: New York.
15. Hudec, P., Smieskova, P., Zidek, Z., Schneider, P., and Solcova, O. (2002) Determination of microporous structure of zeolites by t-plot method. State of the art. In *Studies in Surface Science and Catalysis 142*; Aiello, R., Giordano, G. and Testa, F. (eds.); Elsevier: Amsterdam, The Netherlands.

16. Stoeckli, F., Lavanchy, A., and Hugi-Cleary, D. (1998) Dubinin's theory: A versatile tool in adsorption science. In *Fundamentals of Adsorption VI*. Meunier, F.A. (ed.); Elsevier: Amsterdam, The Netherlands.
17. Lastoskie, C., Gubbins, K.E., and Quirke, N. (1993) Pore size distribution analysis of microporous carbons: a density functional theory approach. *J. Phys. Chem.*, 97: 4786.
18. Treacy, M.M.J., Higgins, J.B., and Von Ballmoos, R. (1990) Collection of simulated XRD powder patterns for zeolites. *Zeolites*, 10: 448.
19. Lowell, S. and Shields, J.E. (1991) *Powder Surface Area and Porosity*, 3rd ed.; Chapman & Hall: London, U. K.
20. Sing, K.S.W., Everett, D.H., Haul, R.A.W., Moscou, L., Pierrotti, R., Rouquerol, J., and Siemienieswka, T. (1985) Reporting physisorption data for gas/solid systems. *Pure Applied Chemical*, 57: 603.
21. Hernandez, M.A., Rojas, F., and Corona, L. (2000) Nitrogen sorption characterization of the microporous structure of clinoptilolite-type zeolites. *J. Porous Mater.*, 7: 443.
22. Hong, Y. and Fripiat, J. (1995) Microporous characteristics of H-Y, H-ZSM-5 and H-mordenite dealuminated by calcination. *J. Microporous Materials*, 4: 323.
23. Carvalho, A.P., Brotas de Carvalho, M., and Pires, J. (1997) Degree of crystallinity of dealuminated offretites determined by X-ray diffraction and by a new method based on nitrogen adsorption. *Zeolites*, 19: 382.
24. Lecloux, A. and Pirard, J.P. (1979) The importance of standard isotherms in the analysis of adsorption isotherms from determination the porous texture of solids. *J. Colloid Interface Sci.*, 70: 265.
25. Kaneko, K. (1994) Heterogeneous Surface Structures of Adsorbents. In *Equilibrium and Dynamics of Gas Adsorption on Heterogeneous Solid Surfaces*; Rudzinski, W., Steele, W., and Zgrablich, G. (eds.); Elsevier: Amsterdam, The Netherlands.
26. Yamanaka, S., Malla, P.B., and Komarneni, S. (1989) Water sorption and desorption isotherms of some naturally occurring zeolites. *Zeolites*, 9: 18.